Available online at www.sciencedirect.com
ScienceDirect
Ceramics International 36 (2010) 1997–2002
CERAMICS INTERNATIONAL
www.elsevier.com/locate/ceramint

Short communication

Effects of impurities on the properties of $BaTiO_3$ synthesized from barium titanyl oxalate

Won-Sik Jung [a], Jiho Park [b], Yunjung Park [b], Dang-Hyok Yoon [a,*]

[a] School of Materials Science and Engineering, Yeungnam University, Gyeongsan 712-749, Republic of Korea
[b] Nano Materials Team, Samsung Fine Chemicals Co., Ltd., Daejeon 305-380, Republic of Korea

Received 20 February 2010; received in revised form 9 March 2010; accepted 23 March 2010
Available online 28 April 2010

Abstract

The effects of impurities, such as H^+/Cl^- and Zr^{4+}, on the tetragonality (=c/a) of $BaTiO_3$ were examined to determine their effect on the synthesis of nano-sized particles with a high dielectric constant. The quantity of incorporated impurities was adjusted by controlling the milling and washing processes, which are essential for the preparation of $BaTiO_3$ using an oxalate method. The tetragonality decreased with increasing impurity concentration, which can be actual proof of the assumption that impurities decrease the tetragonality due to the enhanced internal strain fields. Moreover, the experimental results showing a tetragonality of 1.0068 for a particle size of 119 nm suggest that the dielectric properties of $BaTiO_3$ prepared by the oxalate route may be comparable with those prepared by solid-state reactions by optimizing the process parameters.

Keywords: A. Powders: chemical preparation; B. Impurities; C. Dielectric properties; D. $BaTiO_3$ and titanates

1. Introduction

Nano-sized barium titanate ($BaTiO_3$) particles with a high dielectric constant are preferred for many reasons. However, the ferroelectricity of $BaTiO_3$ decreases with decreasing particle size, and disappears below a critical particle size due to a tetragonal to cubic crystallographic phase transition, which is known as the "size effect" [1,2]. Many attempts have been made to understand this size effect and increase the dielectric constant of the powder whilst maintaining a particle size as small as possible [3–7]. According to the phenomenological surface layer model [8], $BaTiO_3$ particles consist of an outer cubic surface layer with a fixed thickness, a tetragonal core, and a gradual transition layer between these two layers. Since the minimum thickness of the surface cubic layer is approximately 10 nm based on calculations [9,10], a tetragonal $BaTiO_3$ particle that is several tens of nanometers in size is possible theoretically. However, the experimental observations of the critical particle size are generally larger than the theoretical value; ranging from 100 nm to several micrometers [2,11]. This discrepancy has been attributed to the different levels of internal strain energy originating from chemical impurities, grain boundaries, free surfaces, and crystalline defects [12]. It is believed that the inherent strain increases the relative portion of the meta-stable cubic phase in a particle from the viewpoint of the phenomenological surface layer model [2,12].

The XRD pattern for the 44–46° 2θ region has generally been used to estimate the crystallinity of $BaTiO_3$ directly using powder without sintering. Fig. 1 compares a typical XRD pattern of cubic and tetragonal $BaTiO_3$. Cubic $BaTiO_3$ shows a single peak due to the symmetry of the lattice, whereas the tetragonal peak shows peak splitting of the (0 0 2) and (2 0 0) planes in this region. The wide peak separation of the XRD pattern caused by a difference in the lattice parameter is desirable considering that the high dielectric constant of tetragonal $BaTiO_3$ is due to lattice distortion by ionic displacement in the perovskite structure. Therefore, the relative c- to a-axis ratio (=c/a), which is defined as tetragonality, can be used to estimate the dielectric constant of the powder. The other useful parameter that can be obtained from the XRD pattern is the K-factor, which is defined as the relative ratio of the peak intensity of the (2 0 0) plane to the peak intensity of the hollow between the two shoulders (=h_1/h_2), as shown in Fig. 1. The

---

* Corresponding author. Tel.: +82 538102561; fax: +82 538104628.
E-mail address: dhyoon@ynu.ac.kr (D.-H. Yoon).

0272-8842/$36.00 © 2010 Elsevier Ltd and Techna Group S.r.l. All rights reserved.
doi:10.1016/j.ceramint.2010.03.033

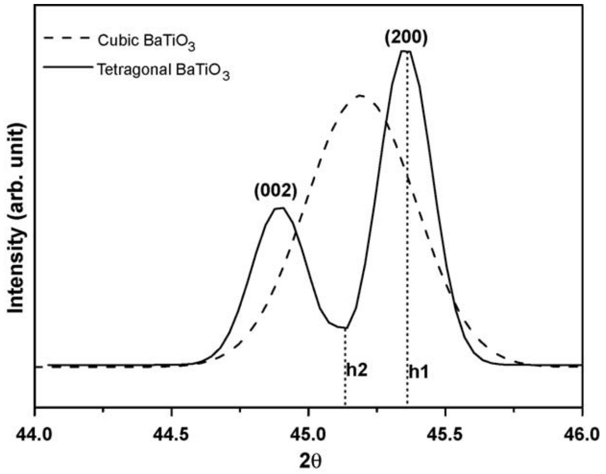

Fig. 1. Typical XRD patterns of cubic and tetragonal $BaTiO_3$ for $2\theta = 44–46^\circ$ [18].

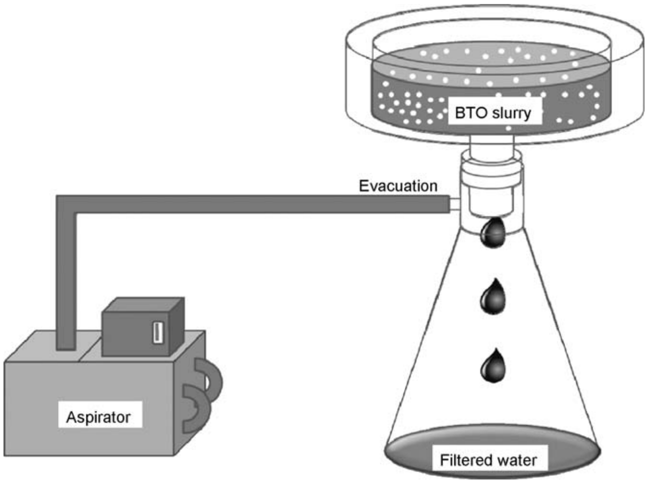

Fig. 2. Schematic diagram of the experimental system for BTO washing using de-ionized water and a filter paper.

K-factor indicates the degree of crystallinity which is the relative ratio of the tetragonal phase to the disordered or cubic portion of the powder.

Although it is believed that impurities stabilize the cubic phase of $BaTiO_3$ due to the strain field and hence decrease the tetragonality, there is no systematic evidence confirming this. Therefore, this study examined the relationship between the tetragonality and impurity levels using $BaTiO_3$ synthesized from barium titanyl oxalate (BTO: $BaTiO(C_2O_4)_2{\cdot}4H_2O$). Two types of inevitable impurities associated with the oxalate method were used as variables: one is a proton (H^+) and/or chlorine ion (Cl^-) originating from the starting materials, and the other is a zirconium ion (Zr^{4+}) from ZrO_2 milling media. When BTO is produced according to the following Eq. (1), H^+ and/or Cl^- ions are present due to incomplete washing.

$$BaCl_2{\cdot}2H_2O + TiOCl_2 + 2H_2C_2O_4{\cdot}2H_2O \rightarrow BaTiO(C_2O_4)_2{\cdot}4H_2O + 4HCl \qquad (1)$$

In addition, contamination from the milling media is always inevitable where the degree of contamination depends on the milling time and type of media. From these perspectives, the dependence of the tetragonality of fine $BaTiO_3$ can be explained in terms of the level of impurities.

2. Experimental procedure

Barium titanyl oxalate (BTO) synthesized from $BaCl_2{\cdot}2H_2O$, $TiOCl_2$ and oxalic acid was obtained from Samsung Fine Chemicals Co., Ltd. The Ba/Ti molar ratio after calcination was 1.000. Eighty grams of BTO mixed with 320 g of de-ionized water were milled using a high-energy mill (MiniCer, Netzsch, Germany) at a rotor speed of 3000 rpm with 0.45 mm ZrO_2 beads. The mean BTO size and corresponding slurry viscosity were measured after different milling times.

Three types of BTO samples were prepared with different impurity levels by changing the milling time and degree of washing. Twelve and 240 min of high-energy milling were performed to prepare BTO containing two different Zr^{4+} contaminant levels associated with milling. The amount of Zr^{4+} was confirmed by X-ray fluorescence (XRF: Simultix 12, Rigaku, Japan). To prepare a sample containing different levels of H^+ and/or Cl^-, the 12 min-milled BTO was washed 10 times with de-ionized water, and filtered through filter paper with a

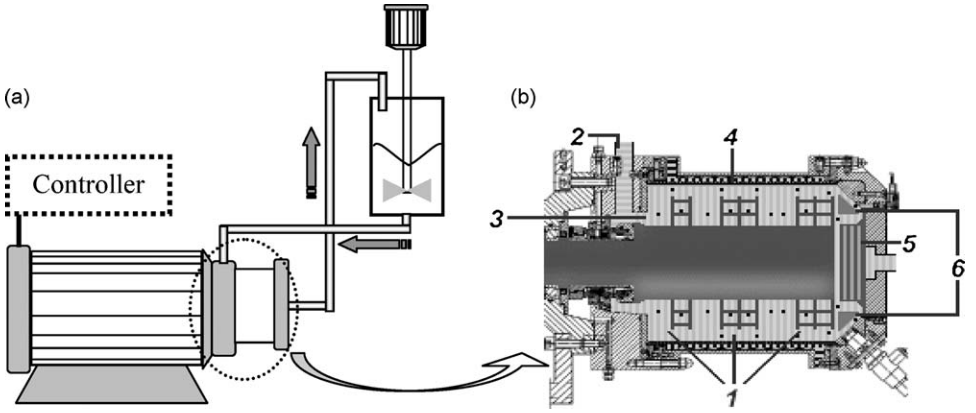

Fig. 3. Schematic diagram of (a) high-energy mill and (b) its milling chamber [13]: 1—rotor with discs; 2—inlet; 3—milling media; 4—cooling jacket; 5 and 6—separation system.

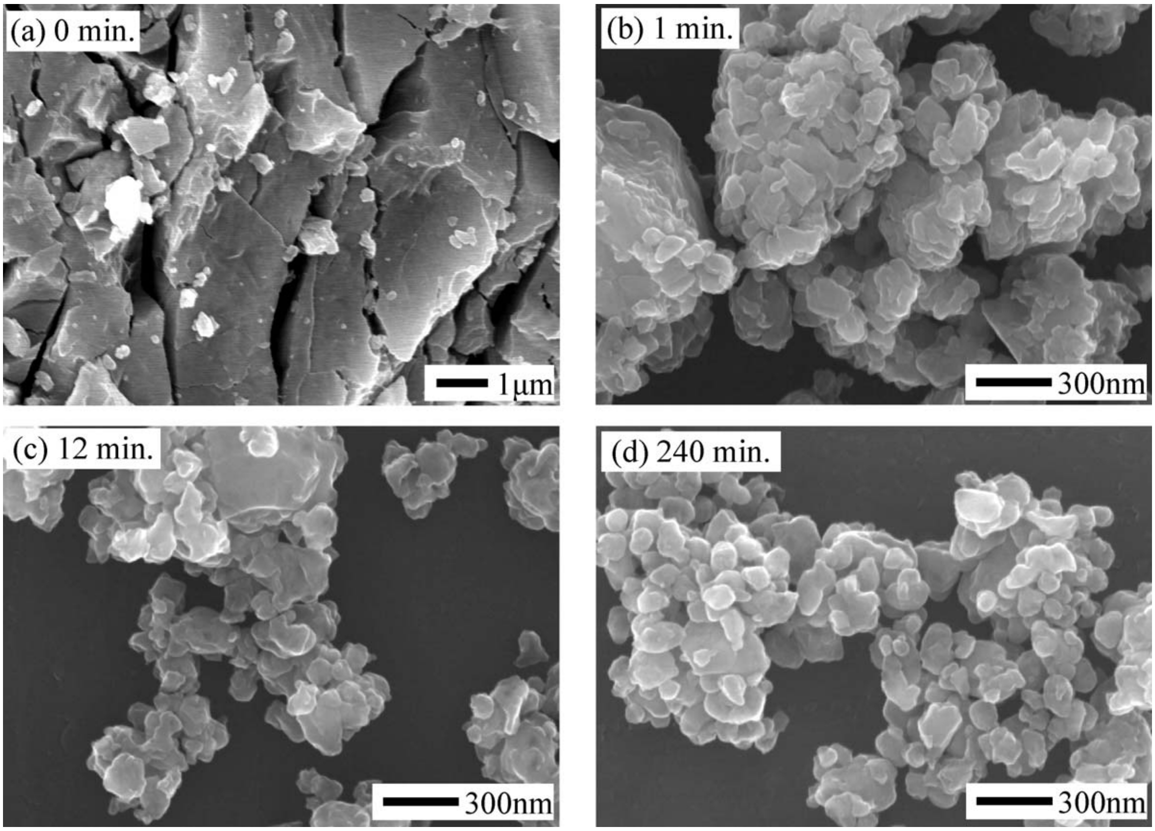

Fig. 4. SEM images of BTO showing the morphological change as a function of the high-energy milling time.

5 μm pore size, as shown in Fig. 2. The change in pH of the filtered water by washing 10 times was monitored to confirm the amount of H^+ in BTO indirectly.

Heat treatment of the above three types of BTO was carried out at 910, 950 and 1010 °C for 3 h at a heating rate of 5 °C/min in air. The change in viscosity of the slurry upon milling was measured at 20 °C using a computer-controlled viscometer (DV-II+ Pro, Brookfield, MA, USA) with a small sample adapter and a SC4-18 spindle at various shear rates. The particle shape and tetragonality of $BaTiO_3$ were determined by scanning electron microscopy (SEM: S-4800, Hitachi using 15 kV, 10 μA and a working distance of 5–8 mm) and X-ray diffraction (XRD: X'Pert-PRO MPD, Panalytical using Cu K_α line, 40 kV and 30 mA), respectively. The mean particle size was estimated from the SEM images by measuring the maximum and minimum diameter of 100 particles using image analyzing software (SigmaScan, Systat Software, USA).

3. Results and discussion

Fig. 3 shows a schematic diagram of the (a) high-energy mill and (b) the grinding chamber of this mill. The milling efficiency

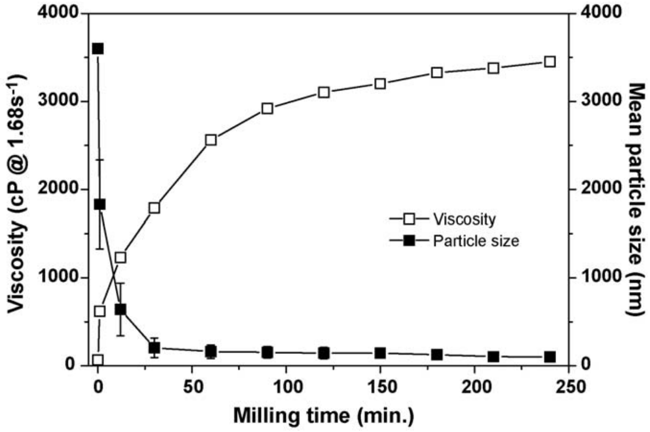

Fig. 5. Evolution of the mean particle size of BTO and the slurry viscosity after high-energy milling.

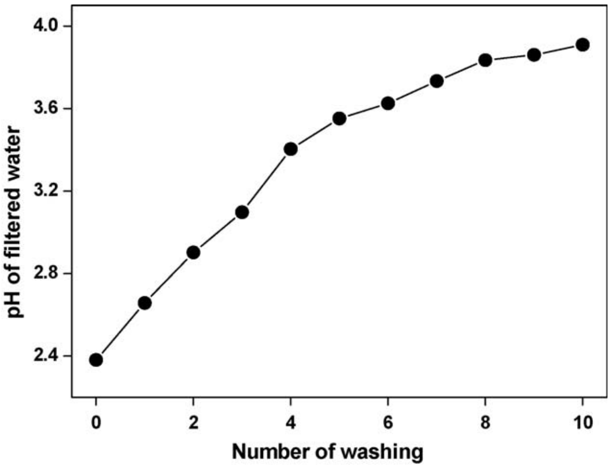

Fig. 6. Change in pH of filtered water as a function of the washing time.

is much higher than that of conventional ball mills because this mill generates a high shear and collision force by rotating up to several thousand rpm equipped with very fine media. Fig. 4 shows SEM images of BTO after different milling times. In contrast to the bulk as-received sample shown in Fig. 4(a), most of the BTO milled into very fine particles after only 12 min milling, even though some coarse particles exist, as shown in Fig. 4(c). All particles after 240 min milling were very fine and showed a uniform size distribution with a mean particle size $\leq$100 nm. Since $BaTiO_3$ is formed by the decomposition of BTO, it can be anticipated that fine BTO will be more desirable for producing small $BaTiO_3$ particles. One example that requires fine $BaTiO_3$ is the multi-layer ceramic capacitor (MLCC), where the thinnest dielectric thickness is currently <1 μm [14,15]. Since 5 grains in each dielectric layer are needed at least to ensure reliability, $BaTiO_3$ $\leq$200 nm with a high dielectric constant is essential. Moreover, the industrial demand will require a particle size of $\approx$100 nm in the near future because of the miniaturization trend in electronics [14,15].

Fig. 5 shows the change in mean BTO size and the viscosity of a slurry as a function of the milling time. The mean particle size and size distribution decreased drastically for the first 30 min of milling and then decreased gradually at a lower rate to 240 min. The viscosity of the slurry increased with increasing milling time because the viscosity is proportional to the surface area created by milling. The 240 min-milled BTO contained 0.998 wt.% zirconium, while the 12 min-milled had

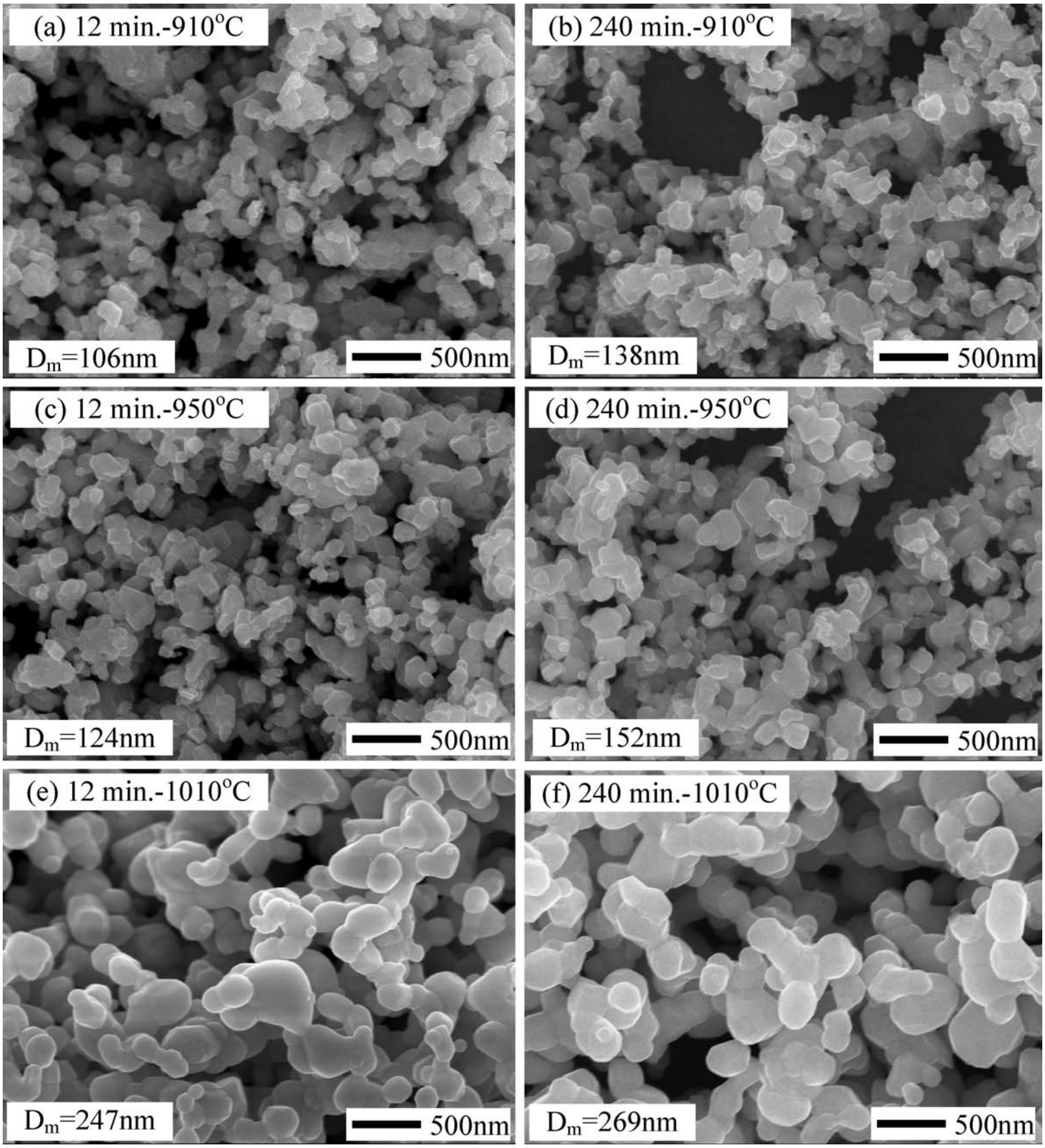

Fig. 7. SEM images of $BaTiO_3$ powder synthesized from BTO for different milling times and calcination temperatures.

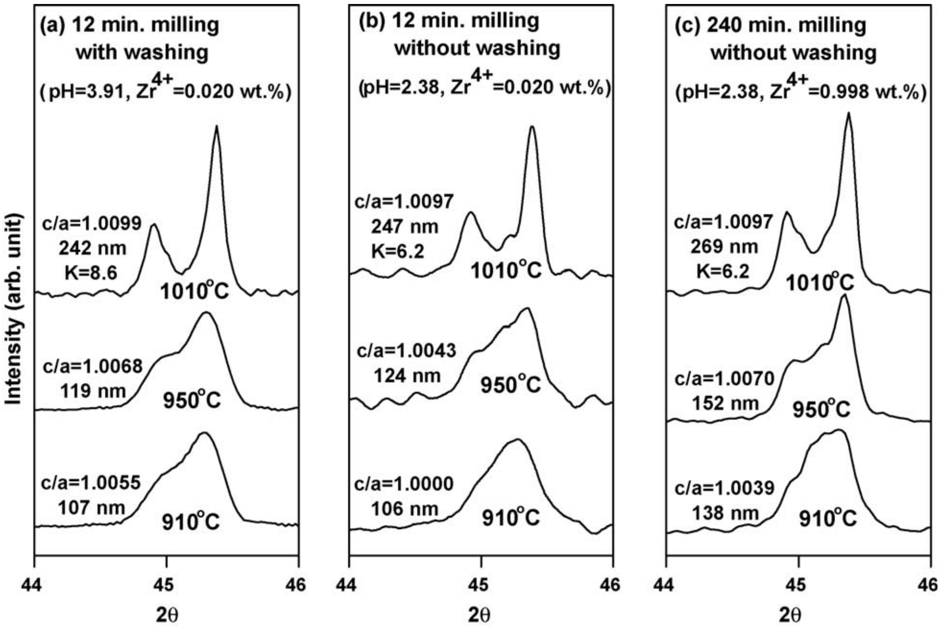

Fig. 8. Comparison of the XRD patterns of $BaTiO_3$ powders synthesized using different milling times, washing and calcination temperatures.

a negligible content of 0.020 wt.% according to XRF. This Zr^{4+} was reported to be incorporated into the Ti^{4+} lattice site of $BaTiO_3$, generating a strain field due to the difference in ionic size (ionic radius for $Zr^{4+} = 0.079$ nm and $Ti^{4+} = 0.068$ nm) [16].

Fig. 6 shows the change in pH of the filtered water during washing 10 times, indicating a gradual increase from 2.38 to 3.91 due to the removal of protons by washing. Although BTO was exposed to washing during the production process, hydrochloric acid (HCl) as a by-product of the oxalic route always remains in BTO due to the incomplete washing, as shown in Eq. (1). Both the retained H^+ and Cl^- are believed to be incorporated into the $BaTiO_3$ lattice as impurities and create a strain field. According to a previous report [17], a hydrothermal powder can contain 40 mol% of protons in the $BaTiO_3$ lattice sites by generating metal ion vacancies for charge compensation. As a result, the suppression of tetragonal distortion in a perovskite unit cell due to the induced strain is expected. Although there is no specific explanation for the effect of Cl^- thus far, it is also believed to deteriorate the tetragonality of $BaTiO_3$ for the same reason. An indirect method of measuring the pH was employed in this study due to the difficulty in quantitative analyzing the Cl^- content in BTO by inductively coupled plasma (ICP) because sample preparation involves the dissolution of the material in HCl.

Fig. 7 shows SEM images of $BaTiO_3$ particles synthesized for two different BTO milling times of 12 and 240 min followed by heat treatment at 910, 950 and 1010 °C for 3 h in air. The mean particle size of $BaTiO_3$ increased with increasing heat treatment temperature, while the BTO milled for 240 min showed a larger particle size than that for 12 min at the same temperature. This was attributed to mechanochemical activation and a finer particle size after a longer milling time, where both can enhance particle growth during heat treatment [18].

Fig. 8 shows the XRD patterns over the range, 44–46° 2θ, of $BaTiO_3$ synthesized by different milling and washing times to determine the relationship between the impurity level and tetragonality. The heat treatment temperature, mean particle size and tetragonality values are also shown in the figure. All the BTO transformed to $BaTiO_3$ at temperatures $\leq$800 °C, even though it is essentially dependent on the sample preparation method. The tetragonality increased with increasing particle size for all cases because the portion of tetragonal phase increased due to the fixed thickness of the surface cubic layer within the framework of the phenomenological surface layer model. Therefore, a comparison of the tetragonality of $BaTiO_3$ particles with similar particle size is desirable to determine the effect of impurities on the tetragonality in 3 cases. $BaTiO_3$ with a lower H^+ and/or Cl^- impurity content shows higher tetragonality than that with a higher content for a similar particle size, as indicated by a comparison of Fig. 8(a) and (b). For example, the tetragonality of the particles prepared without washing increased from 1.0000 and 1.0043 to 1.0055 and 1.0068 after washing the particles heat-treated at 910 and 950 °C, respectively. In addition, the tetragonality decreased with increasing Zr^{4+} content according to a comparison of Fig. 8(c) with Fig. 8(a) and (b). The tetragonality of the 240 min-milled sample containing 0.998 wt.% Zr^{4+} was 1.0039 for a particle size of 138 nm, while the 12 min-milled one with a much lower contaminant concentration of 0.020 wt.% Zr^{4+} was 1.0043 for 124 nm-sized particles. Moreover, $BaTiO_3$ synthesized by 12 min milling, washing and heat treatment at 1010 °C showed the highest *K*-factor of 8.6 compared to the other samples treated at the same temperature, indicating that the *K*-factor can be also increased by decreasing the level of contaminants.

Fig. 9 summarizes the dependence of tetragonality on the particle size of $BaTiO_3$ synthesized with different impurity

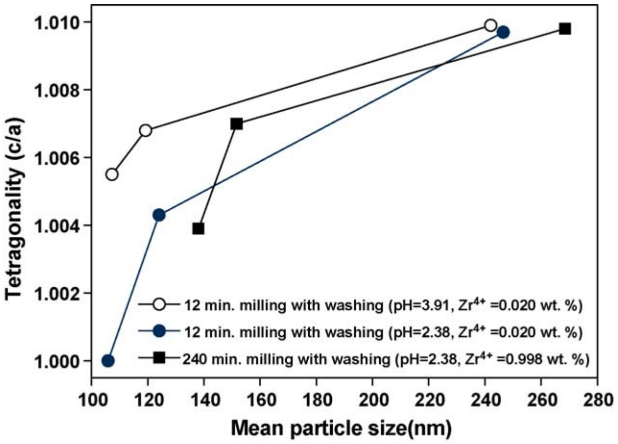

Fig. 9. The relationship between the tetragonality and mean particle size of $BaTiO_3$ powder synthesized for different milling times, washing and calcination temperatures.

levels. Among 3 different sample groups, $BaTiO_3$ powder prepared by 240 min milling without washing showed the fastest decrease in tetragonality with decreasing particle size due to its highest impurity content. On the other hand, $BaTiO_3$ with the lowest impurity content after 12 min milling and washing showed the highest tetragonality, which was due to the smallest strain field originating from the impurities. It is believed that the tetragonality of $BaTiO_3$ prepared by the oxalic method is generally inferior to that by the solid-state method [2,11,18]. However, $BaTiO_3$ containing the lowest level of impurities with a mean particle size of 119 nm showed a tetragonality of 1.0068, which is comparable to that synthesized by the solid-state method. Therefore, minimization of the impurity levels incorporated into $BaTiO_3$ is strongly recommended to meet the industrial demand for a fine particle size with high dielectric properties.

4. Conclusions

The relationship between the impurity levels in $BaTiO_3$ and the resulting tetragonality (=c/a) was explained using two types of inevitable impurities associated with the oxalate route. The amount of Zr^{4+} contaminant in the particle was controlled by varying the milling time, whereas the H^+/Cl^- content was adjusted by BTO washing. Although a longer milling time resulted in finer BTO with a narrower size distribution, the tetragonality of the synthesized $BaTiO_3$ was smaller than that with a shorter milling time due to the increased internal strain field by Zr^{4+}, which stabilizes the meta-stable cubic phase. At the same time, H^+/Cl^- impurities have a similar effect for the same reason. This finding can be an actual example of the assumption that impurities stabilize the cubic phase due to the strain field, and hence decrease the tetragonality and *K*-factor of $BaTiO_3$. A tetragonality of 1.0068 with a particle size of 119 nm could be obtained by decreasing the impurity content, which satisfies the recent industrial demand. In contrast to the generally held belief, this result provides supportive evidence that the dielectric properties of $BaTiO_3$ prepared by the oxalate method can be comparable to those prepared by the solid-state method simply by minimizing the level of contaminants.

Acknowledgements

This study was supported by Samsung Fine Chemicals Co., Ltd. We would like to thank Nano Materials Team at Samsung Fine Chemicals Co. for BTO preparation and helpful discussions.

References

[1] K. Uchino, E. Sadanaga, T. Hirose, Dependence of the crystal structure on particle size in barium titanate, J. Am. Ceram. Soc. 72 (1989) 1555–1558.
[2] D.H. Yoon, Tetragonality of barium titanate powder for a ceramic capacitor application, J. Ceram. Process. Res. 7 (2006) 343–354.
[3] Y. Terashi, A. Purwanto, W. Wang, F. Iskandar, K. Okuyama, Role of urea addition in the preparation of tetragonal $BaTiO_3$ nanoparticles using flame-assisted spray pyrolysis, J. Eur. Ceram. Soc. 28 (2008) 2573–2580.
[4] C. Ando, H. Kishi, H. Oguchi, M. Senna, Effects of bovine serum albumin on the low temperature synthesis of barium titanate microparticles via a solid state route, J. Am. Ceram. Soc. 89 (2006) 1709–1712.
[5] S.G. Kwon, B.H. Park, K. Choi, E.S. Choi, S. Nam, J.W. Kim, J.H. Kim, Solvothermally synthesized tetragonal barium titanate powders using H_2O/EtOH solvent, J. Eur. Ceram. Soc. 26 (2006) 1401–1404.
[6] Y.S. Malghe, A.V. Gurjar, S.R. Dharwadkar, Synthesis of $BaTiO_3$ powder from barium titanyl oxalate (BTO) precursor employing microwave heating technique, Bull. Mater. Sci. 27 (2004) 217–220.
[7] T. Yan, Z.G. Shen, W.W. Zhang, J.F. Chen, Size dependence on the ferroelectric transition of nanosized $BaTiO_3$ particles, Mater. Chem. Phys. 98 (2006) 450–455.
[8] J.C. Niepce, Surfaces and Interfaces of Ceramic Materials, Kluwer Academic Publisher, Netherlands, 1989, p. 512.
[9] W. Känzig, Space charge layer near the surface of a ferroelectric, Phys. Rev. 98 (1955) 549–550.
[10] K. Ishikawa, K. Nagareda, Size effect on the phase transition in ferroelectric fine-particles, J. Korean Phys. Soc. 32 (1998) S56–S58.
[11] D.H. Yoon, B.I. Lee, $BaTiO_3$ properties and powder characteristics for ceramic capacitors, J. Ceram. Process. Res. 3 (2002) 41–47.
[12] S. Wada, T. Hoshina, H. Yasuno, M. Ohishi, H. Kakemoto, T. Tsurumi, M. Yashima, Advances in Electronic Ceramic Materials: Ceramic Engineering and Science Proceedings, American Ceramic Society, USA, 2005, p. 89.
[13] Web-site of "Chicago Boiler Company". http://www.cbmills.com.
[14] T. Tsurumi, T. Sekine, H. Kakemoto, T. Hoshina, S.-M. Nam, H. Yasuno, S. Wada, Evaluation and statistical analysis of dielectric permittivity of $BaTiO_3$ powders, J. Am. Ceram. Soc. 89 (2006) 1337–1341.
[15] H. Kishi, Y. Mizuno, H. Chazono, Base-metal electrode-multilayer ceramic capacitors: past, present and future perspectives, Jpn. J. Appl. Phys. 42 (2003) 1–15.
[16] M.T. Buscaglia, V. Buscaglia, M. Viviani, P. Nanni, M. Hanuskova, Influence of foreign ions on the crystal structure of $BaTiO_3$, J. Eur. Ceram. Soc. 20 (2000) 1997–2007.
[17] D.F.K. Hennings, C. Metzmacher, B.S. Schreinemacher, Defect chemistry and microstructure of hydrothermal barium titanate, J. Am. Ceram. Soc. 84 (2001) 179–182.
[18] J.H. Kim, W.S. Jung, H.T. Kim, D.H. Yoon, Properties of $BaTiO_3$ synthesized from barium titanyl oxalate, Ceram. Int. 35 (2009) 2337–2342.